ChemComm

Chemical Communications

www.rsc.org/chemcomm

Number 36 | 28 September 2008 | Pages 4221–4368

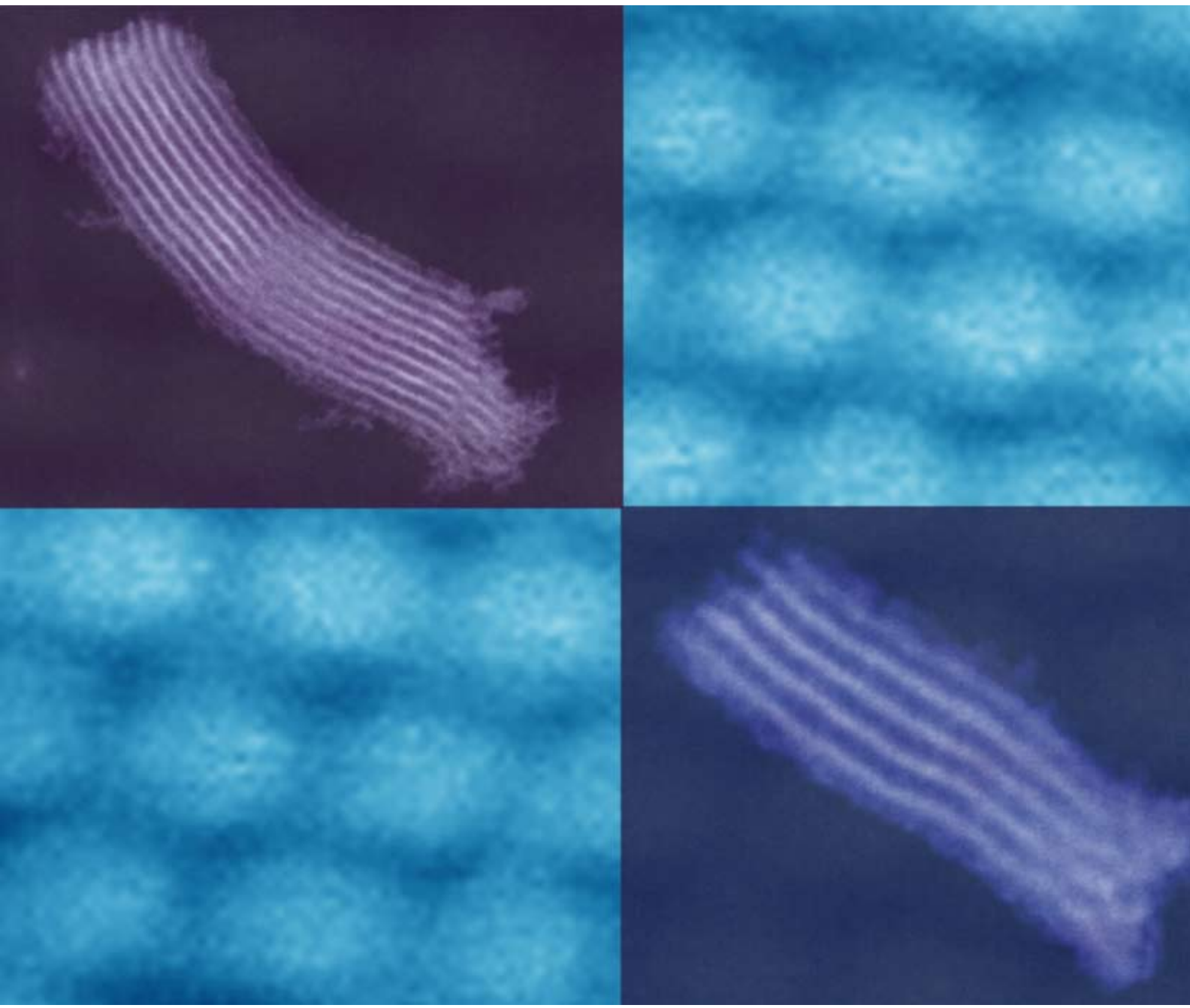

ISSN 1359-7345

RSC Publishing

1359-7345(2008)36;1-Y

Strategic synthesis of SBA-15 nanorods†

Xiulei Ji, Kyu T. Lee, Muguette Monjauze and Linda F. Nazar*

Received (in Cambridge, UK) 19th March 2008, Accepted 14th May 2008
First published as an Advance Article on the web 20th June 2008
DOI: 10.1039/b804327b

A simple synthesis of homogeneously sized, ordered mesoporous silica nanorods (SBA-15), spanning about 10 porous channels in width and ranging from 300 to 600 nm in length is reported.

Periodic mesoporous materials have sparked great research interest since the discovery of the M41S family,[1] and extensive efforts have been devoted to their morphological control.[2] Recently, increasing attention has focused on controlling the morphology of SBA-15. This material has many highly desirable characteristics such as an adjustable large pore size, sturdy walls and an interconnected quasi-2D hexagonal mesostructure (*p6mm*).[3] Many forms of mesoporous silicates closely related to SBA-15 have been obtained by utilizing block copolymers as templates, including fibers,[4] spheres,[5] crystals,[6] monoliths,[7] and ultra-thin platelets.[8] To render the pores of SBA-15 more accessible for guest molecules in various applications, it is crucial to decrease its particle size to shorten the diffusion path length. Discrete rod-like particles of SBA-15 (*ca.* 1.5 × 1 μm) have been obtained in the presence of KCl by Zhao *et al.*[9] Sayari *et al.* have introduced an elegant synthesis of monodispersed SBA-15 rods with uniform size (*ca.* 1.5 × 0.4 μm) under static conditions without any additives,[10] although the mechanism of particle size control was not detailed. The particle growth process has been examined by several *in situ* techniques that probe the mechanism. According to these studies, wormlike nano-domains are proposed to form first, which then interconnect into larger particles (more than 1 μm) after a period of time (60 to 100 min).[11–13] Nonetheless, almost all syntheses of SBA-15 in the past decade were carried out with a similar P123 ($EO_{20}PPO_{70}EO_{20}$) concentration in the reaction mixture of 2.5–3 wt%. Here, we present a simple synthesis of SBA-15 nanodimensioned rods (*ca.* 0.5 × 0.1 μm) that employs a dilute solution of P123 and TEOS in an acidic aqueous medium under static conditions without any additives. This enables us to halt the synthesis at the initial stage in the nucleation and growth mechanism, and thus trap nanorods with particle sizes many orders of magnitude smaller than previously reported. Our studies moreover lend strong support to the proposed microstructure evolution theories based on cryo-TEM, and SAXS/XRD studies.[11–13]

In a typical synthesis, 2 g of Pluronic P123 were dissolved in 360 ml of 2 M HCl at 38 °C. Tetraethyl orthosilicate (TEOS, 4.2 g) was added into the above solution with vigorous stirring. The concentrations of P123 and TEOS in the solution were 0.53 wt% and 1.1 wt%, respectively, ~1/5 of those in conventional syntheses of SBA-15 reported in the literature.[10–13] The mixture was stirred for 6 min and remained quiescent for 24 h at 38 °C. It was subsequently heated at 100 °C for another 24 h in an autoclave. The as-synthesized SBA-15 was collected by centrifugation, dried and calcined at 550 °C in air (yield: 91% based on Si). A series of varying concentrations of P123 and TEOS in 2 M HCl were prepared, with the ratio between P123 and TEOS kept the same as above. These were 1/1, 2/5, 1/5, and 1/10 of the concentrations of P123 and TEOS employed in a conventional synthesis of SBA-15. We refer to these SBA-15 materials as SBA15-1/1, SBA15-1/2.5, SBA15-1/5, and SBA15-1/10.

The declining trend in particle size along the series from SBA15-1/1 to SBA15-1/5 is evident in the microscopy images shown in Fig. 1a–d, and from the data summarized in Table 1. SBA15-1/5 exhibits the smallest particle size along with very uniform morphology, shown in the scanning electron microscopy (SEM) image (Fig. 1a). A survey of the entire sample revealed a remarkably homogeneous particle size distribution that was confirmed by particle size analysis. The diameter of the rods is less than 100 nm, almost 1/15 of SBA15-1/1

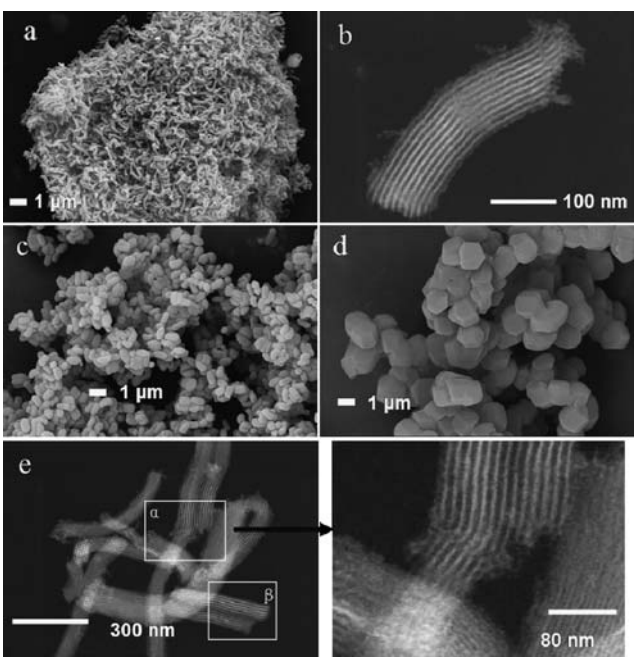

Fig. 1 SEM images of (a) SBA15-1/5, (c) SBA15-1/2.5, (d) SBA15-1/1 recorded on a LEO 1530 field emission SEM instrument, and TEM images of SBA15-1/5, (b) and (e) recorded on a Hitachi HD-2000 STEM.

University of Waterloo, Department of Chemistry, Waterloo, Ontario, Canada N2L 3G1. E-mail: lfnazar@uwaterloo.ca
† Electronic supplementary information (ESI) available: Experimental details. See DOI: 10.1039/b804327b

Table 1 Physical characteristics of mesoporous silicate samples

Samples	Dimensions/μm	$S_{BET}/m^2\ g^{-1}$	$V_p/cm^3\ g^{-1}$	Pore size/nm	d_{100} spacing/nm	Wall thickness/nm
SBA15-1/1	*ca.* 1.5 × 1.2	601	0.83	5.4	8.6	4.5
SBA15-1/2.5	*ca.* 0.8 × 0.5	769	1.06	6.3	10.2	5.4
SBA15-1/5	*ca.* 0.5 × 0.1	619	1.13	6.2	10.5	5.9
SBA15-1/10	*ca.* 0.5 × 0.1	479	0.73	6.5	10.8	6.0
Calcined SBA15-1/5 at 900 °C	*ca.* 0.5 × 0.1	217	0.39	4.3	9.6	6.7
Calcined SBA15-1/1 at 900 °C	*ca.* 1.5 × 1.2	35	0.15	N/A	N/A	N/A

(Fig. 1d). Each nanorod thus spans only ~10 mesoporous silica channels. The length of the rods ranges from 300 nm to 600 nm. Even though the particle size is dramatically decreased, SBA15-1/5 still exhibits highly ordered hexagonal (*P6mm*) symmetry, as seen in the powder X-ray diffraction (XRD) pattern (Fig. 2a,ii) and the transmission electron microscopy (TEM) image (Fig. 1b). The ordered channels are oriented along the long axis of the rod. The morphology of SBA15-1/10 is quite similar to that of SBA15-1/5. SBA15-1/10, prepared with extremely low concentrations of P123 and TEOS, also still exhibits long range order, as shown by the XRD pattern (Fig. 2a,iii). This is in contrast to previous reports that claimed when the concentration of copolymer is lower than 0.5 wt%, only amorphous silica is formed.[3] Similar to nanocrystals with short range order, smaller particles with long range order will also result in less well defined X-ray diffraction peaks since the effective coherence length is reduced.[14] An estimate of the width of the SBA15-1/5 nanocrystallite rods (*i.e.*, domain size) was obtained from analysis of the first reflection in the XRD pattern (100) using the Scherrer equation. The calculated dimension was 87 nm, in excellent accord with the rod width observed in the TEM images of about 90 nm (Fig. 1b and e) that spans an average of 10 porous channels. The corresponding value for SBA15-1/10 was only 49 nm. This follows the same trend as the particle size observed in TEM, and further supports our claim of the order being preserved even at these extremely small length scales.

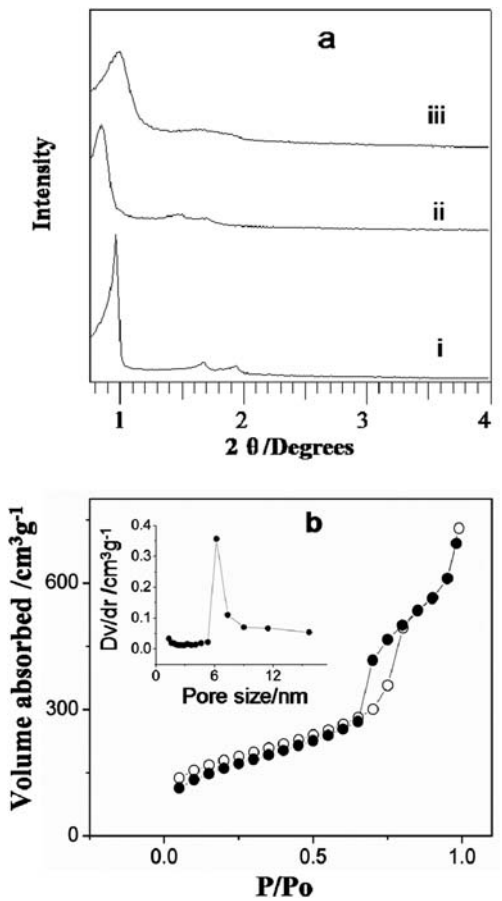

Fig. 2 (a) XRD patterns of (i) SBA15-1/1, (ii) SBA15-1/5, (iii) SBA15-1/10; (b) N_2 adsorption–desorption isotherm for SBA15-1/5. (Inset) Pore size distribution of SBA15-1/5.

The slower rate of nucleation and growth in dilute solution has an effect on the physical characteristics of the materials. Nitrogen adsorption and desorption isotherms were measured for calcined samples, and a typical curve is shown in Fig. 2b for SBA15-1/5. The pore size was determined from the desorption branch, and the resultant physical characteristics of the samples are presented in Table 1. The pore dimensions of all of the series (5.4–6.2 nm) are typical of SBA-15.[3] Compared to SBA15-1/1, all of the series SBA15-1/2.5, SBA15-1/5 and SBA15-1/10 have a larger *d*-spacing and pore size, and thicker walls, the latter being presumably a result of the slower rate process during nucleation. We note that the calculated wall thickness of SBA15-1/5 is consistent with estimation from the TEM images. As a consequence, SBA15-1/5 also exhibited better thermal stability compared to SBA15-1/1. After calcination at 900 °C for 2 h, SBA15-1/5 still maintained appreciable surface area, pore volume and long range order, the latter being confirmed by well defined peaks in the XRD pattern. In contrast, SBA15-1/1 suffered pore collapse. The characteristics of the high temperature calcined samples are shown in Table 1.

We believe that the key to control the particle size of mesoporous silicates is to minimize the chances of collision of the nano-domains formed at an early stage of cooperative assembly/condensation. Fig. 3 depicts the difference between the conventional case and the highly dilute case in terms of the degree of particle growth. In a highly dilute reaction environment, the newly formed wormlike nano-domains are kinetically inhibited from forming larger agglomerates. This is evident in Fig. 1e, where only a few particles are partially connected end to end (inset α) and side to side (inset β). This indicates that the merging of these nanorods is not complete even under hydrothermal conditions owing to the slower rate of nucleation and growth. The very small particle size gives rise to formation of a stable, completely non-settling milky suspension $\frac{1}{2}$ h after the TEOS was added, necessitating material recovery by centrifugation. Under conventional conditions, the nano-domains are closely distributed and rapidly agglomerate into large particles owing to driving forces that minimize surface free energy. In accord, for SBA15-1/1 and

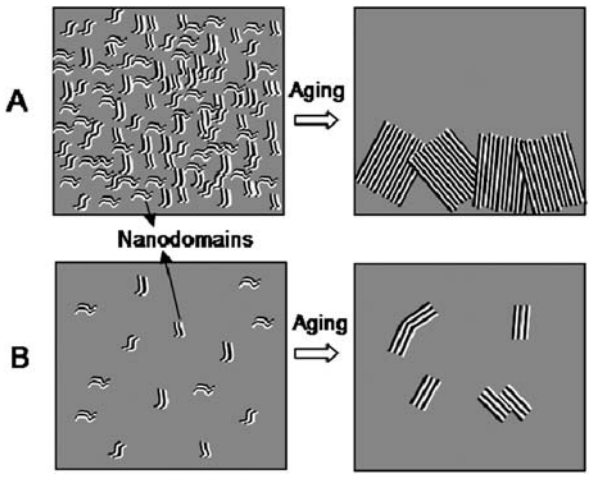

Fig. 3 Schematic diagram depicting the influence of dilution of reaction solution on particle growth. (A) conventional synthesis, (B) highly dilute case.

SBA15-1/2.5, the cloudy suspension appeared in half the time after the addition of TEOS, followed by rapid precipitation.

In summary, we have prepared and characterised mesoporous silica with a novel nano-rod morphology. To our knowledge, this is the first example of such a confined organization of silica channels, whose formation under the controlled conditions we have implemented supports previously proposed mechanisms of growth and nucleation. We note that hexagonal platelets of amino functionalised SBA-15 with short 1D channels have also been realised by chemical modification.[15] According to our preliminary results, this dilution strategy can be applied to other syntheses of mesostructured materials employing amphiphilic molecules and/or copolymers as structure directing agents. We will report those results in a forthcoming paper. The concept of controlled assembly of precursors to form nanotubes is also believed to be responsible for the the synthesis of ultra-short ($\sim$20 nm) aluminium-germanium-hydroxide nanotubes under pH control.[16] The decrease of rod diameter/lengths to nanodimensions is especially important for catalytic inorganic oxide materials that rely on short diffusion lengths,[16,17] and replica template mesoporous materials. These have applications such as conductive scaffolds to encapsulate materials for electrodes in Li ion batteries, more efficient catalyst support materials for PEM fuel cells, and absorption materials for toxic hydrophobic organic molecules for environmental protection. Further work is ongoing in our laboratory to explore such materials.

LFN thanks NSERC (Canada) for its generous support through the Discovery Grant program.

Notes and references

1 C. T. Kresge, M. E. Leonowicz, W. J. Roth, J. C. Vartuli and J. S. Beck, *Nature*, 1992, **359**, 710.
2 H. Yong, N. Coombs and G. Ozin, *Nature*, 1997, **386**, 692.
3 D. Zhao, J. Feng, Q. Huo, N. Melosh, G. H. Fredrickson, B. F. Chmelka and G. D. Stucky, *Science*, 1998, **279**, 548.
4 P. Yang, D. Zhao, B. Chmelca and G. D. Stucky, *Chem. Mater.*, 1998, **10**, 2033.
5 C. Boissiere, A. Larbot, A. van der Lee, P. J. Kooyman and E. Prouzet, *Chem. Mater.*, 2000, **12**, 2902.
6 C. Yu, B. Tian, J. Fan, G. D. Stucky and D. Zhao, *J. Am. Chem. Soc.*, 2002, **124**, 4556.
7 P. Feng, X. Bu, G. D. Stucky and D. J. Pine, *J. Am. Chem. Soc.*, 2000, **122**, 994.
8 Q. Hu, R. Kou, J. Pang, T. Ward, M. Cai, Z. Yang, Y. Lu and J. Tang, *Chem. Commun.*, 2007, 601.
9 C. Yu, J. Fan, B. Tian and D. Zhao, *Chem. Mater.*, 2004, **16**, 889.
10 A. Sayari, B. Han and Y. Yang, *J. Am. Chem. Soc.*, 2004, **126**, 14348.
11 K. Flodström, C. Teixeira, H. Amenitsch, V. Alfredsson and M. Lindén, *Langmuir*, 2004, **20**, 4885.
12 S. Ruthstein, J. Schmidt, E. Kesselman, Y. Talmon and D. Goldfarb, *J. Am. Chem. Soc.*, 2006, **128**, 3366.
13 K. Flodström, H. Wennerstrom and V. Alfredsson, *Langmuir*, 2004, **20**, 680.
14 X. Ji, S. Herle, Y. Rho and L. F. Nazar, *Chem. Mater.*, 2007, **19**, 374.
15 S. Sujandi, S.-E. Park, D.-S. Han, S.-C. Han, M.-J. Jin and T. Ohsuna, *Chem. Commun.*, 2006, 4131.
16 S. Mukherjee, K. Kim and S. Nair, *J. Am. Chem. Soc.*, 2007, **129**, 6820.
17 S. Nair, L. Villaescusa, M. Camblor and M. Tsapatsis, *Chem. Commun.*, 1999, 921.

